

Preprint of

N. Éber, P. Salamon and Á. Buka: Competition between Electric Field Induced Equilibrium and Non-Equilibrium Patterns at Low Frequency Driving in Nematics. In *Proceedings of the 13th Small Triangle Meeting on Theoretical Physics*, Stará Lesná, November 14-16, 2011, J. Buša, M. Hnatič and P. Kopčanský (eds.), IEP SAS, Košice, 2012, pp. 56-63.

Erratum

The legend in Fig. 2b has unfortunately been mistyped.
Correctly the black dotted line corresponds to the conductive EC, while the solid red line belongs to the dielectric EC.



Competition between Electric Field Induced Equilibrium and Non-Equilibrium Patterns at Low Frequency Driving in Nematics

N. Éber, P. Salamon, Á. Buka

*Institute for Solid State Physics and Optics,
Wigner Research Centre for Physics,
Hungarian Academy of Sciences,
H-1525 Budapest, P.O.Box 49, Hungary*

Abstract

We studied the temporal evolution of electric field induced patterns in the nematic Phase 5 in a wide driving frequency range. The compound exhibits a transition from conductive to dielectric regime of electroconvection (EC) at high frequency. At low frequencies we found that the conductive EC rolls evolve and decay in each half period of driving. Following EC rolls another pattern, flexoelectric domains (FD), also appear as flashes in the same half period. This scenario thus represents a repetitive morphological transition between dissipative (EC) and equilibrium (FD) patterns.

Introduction

Nematic liquid crystals are anisotropic fluids possessing long-range orientational order, characterised by the averaged direction of the long axes of their rod-like molecules, called the director \mathbf{n} . Spatial variation of \mathbf{n} leads to an elastic free energy of the system [1]:

$$F_K = \int \rho \left\{ \frac{1}{2} K_1 (\nabla \cdot \mathbf{n})^2 + \frac{1}{2} K_2 (\mathbf{n} \cdot \nabla \times \mathbf{n})^2 + \frac{1}{2} K_3 (\mathbf{n} \times \nabla \times \mathbf{n})^2 \right\} dV. \quad (1)$$

The coefficients K_1 , K_2 and K_3 are elastic moduli belonging to the three basic deformation types: splay, twist and bend, respectively.

The orientation of nematics may be affected by electric fields due to the anisotropy of their dielectric permittivity, $\epsilon_a = \epsilon_{\parallel} - \epsilon_{\perp}$, where ϵ_{\parallel} and ϵ_{\perp} denote the permittivities measured along and normal to \mathbf{n} , respectively. In addition to that, an orientational deformation (director gradient) may induce a so-called flexoelectric polarisation [1, 2], $\mathbf{P}_{fl} = e_1 \mathbf{n} (\nabla \cdot \mathbf{n}) - e_3 (\mathbf{n} \times \nabla \times \mathbf{n})$, (e_1 and e_3 are flexoelectric coefficients). The interaction of the dielectrically and flexoelectrically

induced polarisations with the electric field \mathbf{E} yields another contribution to the free energy of the system:

$$F_E = \int \rho \left\{ -\frac{1}{2} \epsilon_0 \epsilon_a (\mathbf{n} \cdot \mathbf{E})^2 - \mathbf{P}_{fl} \cdot \mathbf{E} \right\} dV. \quad (2)$$

Liquid crystals are typically studied in a sandwich cell geometry, i.e. confined between two glass substrates (x - y plane) coated with transparent conductive electrodes, allowing to create an electric field along z by applying a voltage. By special surface treatments one can assure a fixed boundary condition for the director, e.g. being parallel with the substrate; in the following we will assume exclusively such a planar surface orientation with \mathbf{n} along x .

The equilibrium director distribution in the sample corresponds to the minimum of the total free energy $F = F_K + F_E$. With no voltage applied this usually implies a constant \mathbf{n} defined by the surfaces. Whenever this initial state is not preferred by the electric field, as e.g. in a planar sample of a nematic with $\epsilon_a > 0$, the field induces a rotation of the director in the bulk. One of the simplest manifestation of this effect is the well known splay Freedericksz transition [1], a director tilt homogeneous in the $x - y$ plane, occurring if the applied voltage V exceeds a threshold voltage $V_F = \pi \sqrt{\frac{K_1}{\epsilon_0 |\epsilon_a|}}$. As seen, the threshold does not depend on the flexoelectric coefficients, however, the deformation profile $\mathbf{n}(z)$ does [3].

Under certain, not too frequent, conditions where the flexoelectric energy-gain exceeds the elastic and dielectric increase of the free energy, the initial state becomes destabilized by a spatially periodic director distortion. The resulting pattern appears as stripes running parallel to the initial director, i.e. $\mathbf{n}(y, z) \propto \sin(y)$. This pattern which still represents a flow-less equilibrium deformation, has been coined flexoelectric domains (FD). It was first observed by Vistin [4] and interpreted by Bobilev and Pikin [5] in the 1970s. Its approximate threshold voltage $V_{fl} = \frac{2\pi K}{|\epsilon_1 - \epsilon_3|(1+\mu)}$, calculated assuming $K_1 = K_2 = K_3 = K$ with $\mu = \frac{\epsilon_0 \epsilon_a K}{(\epsilon_1 - \epsilon_3)^2}$, reflects its flexoelectric origin. Recently the description has been improved by including anisotropic elasticity [6], on the expense that no closed formulas could be obtained for the threshold voltage.

Pattern formation in electric field is quite frequent in nematics, however, most of the patterns – in contrast to the flexo-domains – are of dissipative character [8]. Those patterns are characterized, besides the spatially modulated director, by flow vortices and periodic space charge distribution. Interpretation of these phenomena, usually called electroconvection (EC), require more sophisticated theoretical description: torque balance equations for the director, anisotropic Navier-Stokes equations for the flow, Maxwell's equations for the charge distribution. The combination of these equations supplemented with the assumption of Ohmic electrical conductivity forms the standard model (SM) of EC [7], which could provide the onset characteristics (threshold voltages and critical wave vectors) of the most common variety of EC patterns (the standard EC) occurring in nematics with specific material parameter combinations. Recent extension of the SM by inclusion of flexoelectricity [9] not only improved the onset predictions, but offered a driving mechanism for non-standard EC patterns detected in another class of nematics.

Concerning experimental observability, flexo-domains are generated by DC or low frequency (below a few Hz) AC voltages in a few nematic compounds. Electroconvection is more frequent among nematics; moreover, it may occur in much wider frequency range, from DC up to several ten kHz AC driving, though has mostly been studied experimentally for $10 \text{ Hz} < f < 1 \text{ kHz}$. In the rare cases, however, where both types of pattern occur in the same compound, the frequency range of their existence is mostly well separated.

In this paper we present a study of pattern formation in a nematic compound which exhibits both FD and standard EC patterns. We extend the f range of the excitation to unusually low frequencies (down to 10 mHz). First, we will show that at such an ultra-low frequency, in contrast to the high f behaviour, a pattern exists in the form of flashes, in a small part of the driving period only. Second, we prove that EC and FD can exist alternately at the same voltage and frequency, producing a repetitive morphological transition. Third, we will analyse how the transition from the high f to low f behaviour occurs in the EC patterns at varying the frequency.

Samples and Methods

Experiments were carried out in a commercial, room temperature nematic mixture, Phase 5 (Merck). It has negative dielectric and positive conductivity anisotropies, a proper combination for the occurrence of standard electroconvection.

The measuring set-up was built around a polarising microscope which was equipped with a high-speed digital camera, capable to record a sequence of about 4000 images of 512×512 pixels at a variable (maximum 2000 frames/s) speed. Planar aligned samples of $d = 11.4 \mu\text{m}$ thickness were tested at $T = 30.0 \pm 0.05 \text{ }^\circ\text{C}$ using the shadowgraph (single polarizer) technique. Sinusoidal AC voltages of rms value V have been applied to the cell through a high voltage amplifier. For proper monitoring of the temporal behaviour within a driving period of the voltage, the start of recording of the image sequences was synchronized with the negative zero crossing of the voltage applied to the cell.

The digital recording of image sequences has dual advantages. First, it allows replay at a modified (slower or faster than real time) speed for easier comparison of recordings at different f . Second, a digital processing allows to quantify the strength of the pattern by a proper contrast (C) definition. In the paper we will identify C with the square deviation from the average image intensity. With this definition the initial undistorted state still has a non-zero contrast value (C_0) which originates from thermal fluctuations or alignment defects.

Morphological transitions at varying the frequency

Applying an AC voltage to the sample standard EC patterns could be observed in the whole studied frequency range. Figure 1 shows the frequency dependence of the threshold voltages. For $f > 10 \text{ Hz}$ the usual monotonic increase of V_c was found with a change in the slope of $V_c(f)$ at $f_c = 230 \text{ Hz}$ indicating a morphological

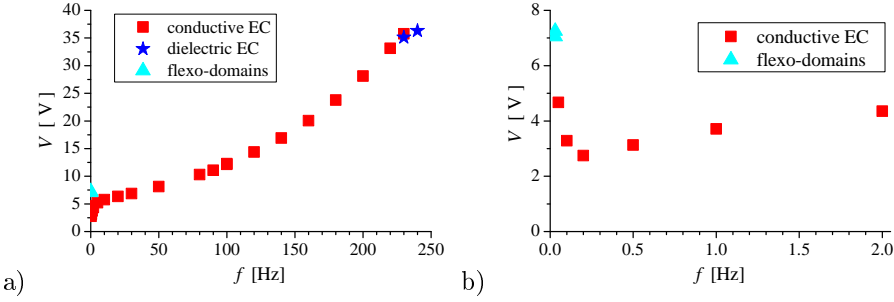


Figure 1: a) Frequency dependence of the threshold voltage for pattern onset; b) the low frequency part of the same dependence.

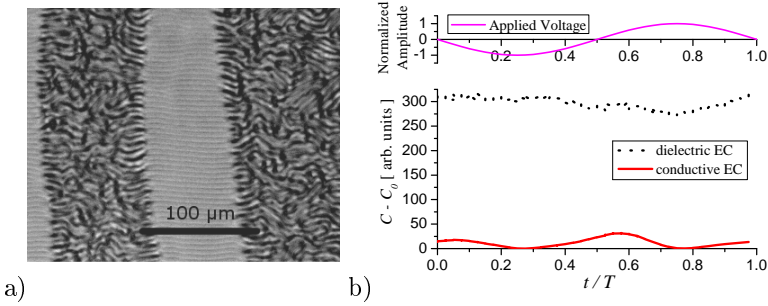


Figure 2: a) Snapshot of dielectric and conductive EC patterns coexisting in patches; b) Temporal evolution of the background subtracted contrast in the dielectric and the conductive patches, respectively.

transition between two EC regimes, the conductive (at lower f) and the dielectric (at high f) ones. According to the SM of EC the two regimes differ, besides in the wavelength of the patterns, in their temporal symmetry; the director is nearly stationary in the conductive regime, but oscillates with the frequency of the driving voltage in the dielectric regime.

Accidentally it may happen that conductive and dielectric rolls can be observed simultaneously in separate patches, as shown in Fig. 2a. This scenario may occur in an inhomogeneous sample where some material parameters (assumably the conductivity) and consequently the crossover frequency differ in the neighbouring patches. The straight horizontal rolls in Fig. 2a running normal to \mathbf{n}_0 represent the dielectric EC regime slightly above the threshold in a patch with $f > f_{c1}$. In the other patch $f < f_{c2}$; thus we see a conductive EC. In that region, however, V_c is considerably lower; therefore the pattern shown is much above the threshold, as indicated by the curved, defect-rich roll structure of high contrast.

This scenario allows a direct comparison of the temporal behaviour of the two EC regimes. Fig. 2b exhibits the temporal evolution of the contrast for the conductive as well as for the dielectric patches. It is immediately seen that the contrast of the conductive rolls remains high and almost constant over the driving period.

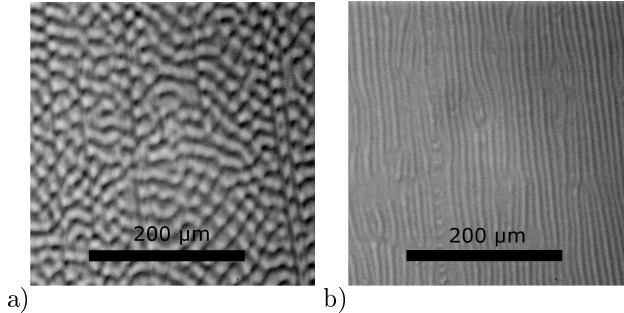


Figure 3: Snapshots of patterns excited by a low frequency ($f = 30$ mHz applied voltage). a) Standard electroconvection (overlapping oblique rolls); b) flexo-domains (parallel stripes). The EC and FD patterns occur successively within the same half period of driving.

Contrary to this behaviour, the contrast of the dielectric rolls is sinusoidally modulated by $2f$ and the contrast minima correspond to the background value. This proves that the dielectric rolls disappear at two time instants in each period, just as it is predicted by the SM.

Let us now focus on the behaviour at low frequencies. The standard conductive EC persists to the low f end of the studied frequency range. Figure 1b depicts the frequency dependence of the threshold voltages exploded for $f < 2$ Hz. It is seen that lowering f the threshold first decreases as reported recently [10], however, reaching a minimum it starts growing as $f \rightarrow 0$. At very low f flexo-domains could also be detected, their threshold is shown in Fig. 1b by triangle symbols. Figure 3 presents snapshots of the two distinct pattern morphologies, conductive EC and FD, at $f = 30$ mHz. We have to emphasize, however, that the snapshots were taken at the same voltage and cell location, but time shifted. Thus the morphological transition between EC and FD occurs here not by changing the control parameters (frequency or voltage) as usual at high f , but at fixed control parameters, repeatedly by time elapsing.

This fact points at a peculiar, surprising feature of the low frequency temporal behaviour of both EC and FD patterns: they exist only in a narrow time window of the driving period as flashes. This feature is illustrated in more detail in Fig. 4a which shows the evolution of the background subtracted pattern contrast within a single driving period. At low voltages there is no pattern, therefore $C - C_0 = 0$. Increasing V first a contrast spike emerges at about $t_1/T = 0.05$, then at higher voltages a second spike develops at about $t_2/T = 0.26$. Comparing with the recorded images it became evident that the first spike (at t_1) corresponds to the EC pattern, while the second (at t_2) belongs to the flexo-domains. It can also be seen in Fig. 4a that the widths of the spikes are quite narrow, i.e. both kinds of patterns decay fully, before the appearance of the other.

The behaviour described above is reminiscent of the low frequency scenarios reported recently [11] for another nematic with a crossover between dielectric EC and FD. However, while the emergence and decay of the dielectric EC pattern

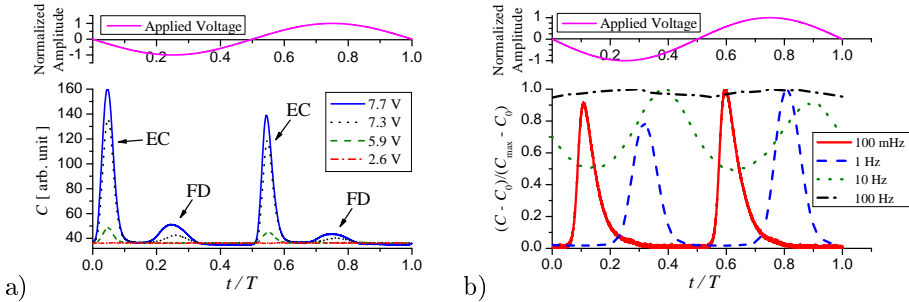


Figure 4: Temporal evolution of the background subtracted contrast within a driving period a) for different applied voltages at $f = 30$ mHz; b) for different frequencies at voltages slightly above onset. The upper graph shows the waveform of the applied voltage.

within each half period of driving was not surprising in [11] since in some sense it occurs also at high f (see e.g. Fig. 2b), the same was not expected for the conductive regime in our case.

It is needless to say that the low f spiky behaviour of conductive EC shown in Fig. 4a does not resemble the stationary high frequency one of the same regime (shown Fig. 2b). Therefore it was necessary to explore, how the transition from one type to the other behaviour occurs at changing f . Figure 4b exhibits the temporal evolution of the background subtracted, normalized contrast for a single period at various driving frequencies. It is noticeable that the almost constant contrast value at $f = 100$ Hz becomes first $2f$ -modulated ($f = 10$ Hz), then the minimum of $C - C_0$ reaches zero and the sinusoidal shape of the modulation transforms into a spiky one at even lower f .

For a more detailed visualization of the transition we have plotted the relative contrast modulation, $(C_{max} - C_{min})/(C_{max} - C_0)$, versus f in Fig. 5a. The nearly zero high f value corresponds to the usual, stationary conductive EC pattern, while in the frequency range of the spikes (low f) the same value increases to 1. The transition between these two regimes occurs continuously in the range of $1 \text{ Hz} < f < 30 \text{ Hz}$ (i.e. $0.03 \text{ s} < T < 1 \text{ s}$). The director relaxation time calculated for the given cell, $\tau_d = 0.147 \text{ s}$, falls within this range, showing that spikes occur at $T \gg \tau_d$.

It can be seen in Fig. 4b that, besides the magnitude of modulation, the positions of the contrast maxima are also frequency dependent. Figure 5b plots these locations versus f . We remind here that $t = 0$ in our figures correspond to the negative zero crossing of the applied voltage (as it can be checked in Fig. 4). It can be seen that the EC contrast maxima typically do not coincide with the location of voltage maxima; at high f they are ahead, while at low f they are behind that. It is also evident from Fig. 5b that at very low f EC spikes appear first after the zero crossing of the applied voltage and that is followed by the FD pattern. Unfortunately FD could be detected only in a quite small frequency range. At

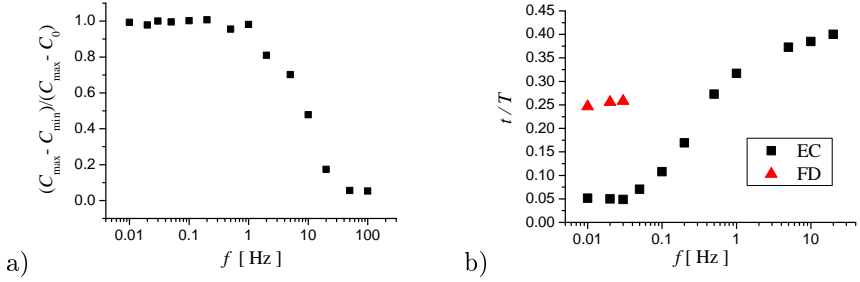


Figure 5: Frequency dependence of a) the relative contrast modulation; b) the positions of contrast maxima within a half period.

higher frequencies the separation between EC and FD reduces and flexo-domains cannot be clearly identified.

Conclusions

In the paper we have provided experimental proofs that the conductive regime of standard electroconvection exhibits unusual scenarios if the nematic is driven by ultra-low frequency ac voltages, which is manifested in the flashing character of the pattern. It has also been shown that a morphological transition, an alternation between conductive EC rolls and flexo-domains, occurs repetitively, in each half period. These features agree well with those found recently for the low f behaviour of dielectric EC [11]. It indicates that at low frequencies conductive and dielectric EC patterns cannot be simply distinguished experimentally by their temporal evolution.

Recent theoretical developments [6] has allowed to calculate the time dependence of the director in EC patterns or flexo-domains. Numerical simulations have confirmed the low f spiky behaviour of both patterns as well as the presence of time shift between EC pattern and flexo-domain spikes. Further experimental and theoretical efforts are required, however, to check whether a quantitative match between theory and experimental data can be obtained.

Acknowledgment

This work was supported by the Hungarian Research Fund under grant OTKA K81250. The authors are grateful for A. Krekhov for illuminating discussions. N.É. thanks for the hospitality provided in the framework of a SAS-HAS bilateral exchange project.

References

- [1] P. G de Gennes, and J. Prost, *The Physics of Liquid Crystals*. (Clarendon Press, Oxford, 1993).
- [2] R. B. Meyer, Piezoelectric effects in liquid crystals, *Phys. Rev. Lett.* **22**(18), 918–921, (1969). doi: 10.1103/PhysRevLett.22.918
- [3] C. V. Brown, and N. J. Mottram, Influence of flexoelectricity above the nematic Freedericksz transition, *Phys. Rev. E* **68**(3), 031702/1–5, (2003). doi: 10.1103/PhysRevE.68.031702
- [4] L. K. Vistin', Electrostructural effect and optical properties of a certain class of liquid crystals and their binary mixtures, *Sov. Phys. Crystallogr.* **15**(3), 514–515, (1970) [*Kristallografiya* **15**(3), 594–595, (1970)].
- [5] Yu. P. Bobilev, and S. A. Pikin, Threshold piezoelectric instability in a liquid crystal, *Sov. Phys. JETP* **45**(1), 195–198, (1977) [*Zh. Eksp. Teor. Fiz.* **72**(1), 369–374, (1977)].
- [6] A. Krekhov, W. Pesch, and Á. Buka, Flexoelectricity and pattern formation in nematic liquid crystals, *Phys. Rev. E* **83**(5), 051706/1–13, (2011). doi: 10.1103/PhysRevE.83.051706
- [7] E. Bodenschatz, W. Zimmermann, and L. Kramer, On electrically driven pattern-forming instabilities in planar nematics, *J. Phys. (France)* **49**(11), 1875–1899, (1988). doi: 10.1051/jphys:0198800490110187500
- [8] L. Kramer, and W. Pesch, *Electrohydrodynamic instabilities in nematic liquid crystals*. In eds. Á. Buka, and L. Kramer, *Pattern Formation in Liquid Crystals*. pp. 221-256. (Springer-Verlag, New York, 1996).
- [9] A. Krekhov, W. Pesch, N. Éber, T. Tóth-Katona, and Á. Buka, Nonstandard electroconvection and flexoelectricity in nematic liquid crystals, *Phys. Rev. E* **77**(2), 021705/1–11, (2008). doi: 10.1103/PhysRevE.77.021705
- [10] T. Tóth-Katona, N. Éber, Á. Buka, and A. Krekhov, Flexoelectricity and competition of time scales in electroconvection, *Phys. Rev. E* **78**(3), 036306/1–12, (2008). doi: 10.1103/PhysRevE.78.036306
- [11] Martin May, Wolfgang Schöpf, Ingo Rehberg, Alexei Krekhov, Agnes Buka, Transition from longitudinal to transversal patterns in an anisotropic system. *Phys Rev E* **78**, 046215 (2008)